

# **FINAL REPORT**

contract order number FA8655-07-M-4015

**Thomas Lippert**  
**Paul Scherrer Institut 5232 Villigen PSI, Switzerland**

Polymers as fuel for Laser Plasma Thrusters: viscous polymers  
and test for nanoparticles emission

REPORT DOCUMENTATION PAGE				Form Approved OMB No. 0704-0188	
Public reporting burden for this collection of information is estimated to average 1 hour per response, including the time for reviewing instructions, searching existing data sources, gathering and maintaining the data needed, and completing and reviewing the collection of information. Send comments regarding this burden estimate or any other aspect of this collection of information, including suggestions for reducing the burden, to Department of Defense, Washington Headquarters Services, Directorate for Information Operations and Reports (0704-0188), 1215 Jefferson Davis Highway, Suite 1204, Arlington, VA 22202-4302. Respondents should be aware that notwithstanding any other provision of law, no person shall be subject to any penalty for failing to comply with a collection of information if it does not display a currently valid OMB control number. <b>PLEASE DO NOT RETURN YOUR FORM TO THE ABOVE ADDRESS.</b>					
<b>1. REPORT DATE (DD-MM-YYYY)</b> 07-01-2008		<b>2. REPORT TYPE</b> Final Report		<b>3. DATES COVERED (From – To)</b> 20 August 2007 - 20-Dec-07	
<b>4. TITLE AND SUBTITLE</b>  Polymers as fuel for Laser Plasma Thrusters: viscous polymers and test for nanoparticles emission			<b>5a. CONTRACT NUMBER</b> FA8655-07-M-4015		
			<b>5b. GRANT NUMBER</b>		
			<b>5c. PROGRAM ELEMENT NUMBER</b>		
<b>6. AUTHOR(S)</b>  Dr. Thomas KM Lippert			<b>5d. PROJECT NUMBER</b>		
			<b>5d. TASK NUMBER</b>		
			<b>5e. WORK UNIT NUMBER</b>		
<b>7. PERFORMING ORGANIZATION NAME(S) AND ADDRESS(ES)</b> Paul Scherrer Institut OFLB U110 Villigen PSI CH-5232 Switzerland				<b>8. PERFORMING ORGANIZATION REPORT NUMBER</b>  N/A	
<b>9. SPONSORING/MONITORING AGENCY NAME(S) AND ADDRESS(ES)</b>  EOARD Unit 4515 BOX 14 APO AE 09421				<b>10. SPONSOR/MONITOR'S ACRONYM(S)</b>	
				<b>11. SPONSOR/MONITOR'S REPORT NUMBER(S)</b> SPC 07-4015	
<b>12. DISTRIBUTION/AVAILABILITY STATEMENT</b>  Approved for public release; distribution is unlimited.					
<b>13. SUPPLEMENTARY NOTES</b>					
<b>14. ABSTRACT</b>  This report results from a contract tasking Paul Scherrer Institut as follows: The Grantee will investigate A.) Ablation of viscous polymers-- Liquid fuels could be used as easy solution to transport sufficient amounts of fuel with a minimum weight of the device. A major issue that has to be controlled is the splashing of the solution during the ablation process, which has been reported to occur during the ablation of liquids. Ns-shadowgraphy measurements on the ablation of viscous polymer solutions will show whether the viscosity has an influence on the splashing behavior.shadowgraphy measurements, B.)Test for emission of nanoparticles--Plasma imaging has shown that the plasma consists of 3 different components which are emitted with different velocities. These different components could be assigned to ions and neutrals (fastest), neutral diatomic species and probably nanoparticles that are emitted at longer time scales (> 200 ns). Additional experiments at these longer timescales with spectral resolution will be used to confirm the existence of the nanoparticles.Until now a clear separation of different components in the plume has not been reported for ns irradiation of polymers. It is therefore of great interest to compare the results obtained for femto- and nanosecond laser irradiation especially whether the component separation and nanoparticles emission is only observed for the ultrashort pulses. Additionally, mass spectroscopy measurements should be performed for nanosecond laser irradiation on the same species that have been observed in the plasma emission spectroscopy measurements. C.) Publication of data.in peer reveiwed journals.					
<b>15. SUBJECT TERMS</b> EOARD, Micro Satellite Technology, laser propulsion, Polymers, laser plasma					
<b>16. SECURITY CLASSIFICATION OF:</b>			<b>17. LIMITATION OF ABSTRACT</b> UL	<b>18, NUMBER OF PAGES</b> 16	<b>19a. NAME OF RESPONSIBLE PERSON</b> BARRETT A. FLAKE
<b>a. REPORT</b> UNCLAS	<b>b. ABSTRACT</b> UNCLAS	<b>c. THIS PAGE</b> UNCLAS			<b>19b. TELEPHONE NUMBER</b> (Include area code) +44 (0)1895 616144

# Table of Content

<b>Table of Content</b>	<b>2</b>
<b>Figures</b>	<b>2</b>
<b>Ablation of viscous polymers</b>	<b>3</b>
<b>Experimental</b>	<b>3</b>
<b>Shadowgraphy</b>	<b>5</b>
Solid GAP	5
Ethyl acetate (solvent with carbon)	6
Non-splashing behavior	7
Splashing behavior	8
Transition between the behaviors	9
Shockwave velocities	11
<b>Carbon nanoparticle during/after plasma formation with fs laser irradiation</b>	<b>13</b>
<b>Preparation of publication from previous project</b>	<b>15</b>

## Figures

Figure 1 : Overview of the experimental setup.	4
Figure 2: Sequence of pictures taken for solid GAP with 1% C particles at $3.2 \text{ J/cm}^2$ .	5
Figure 3: Sequence of pictures taken for ethyl acetate (solvent) with 0.7% C particles at $2.8 \text{ J/cm}^2$ .	6
Figure 4: Sequence of pictures taken for the 70% GAP solution at $2.2 \text{ J/cm}^2$ .	7
Figure 5: Sequence of pictures taken for the 28% GAP solution at $4.5 \text{ J/cm}^2$ .	8
Figure 6: Pictures taken after $9 \mu\text{s}$ with $0.55 \text{ J/cm}^2$ for different GAP concentrations.	9
Figure 7: Pictures taken after $10 \mu\text{s}$ with $0.8 \text{ J/cm}^2$ for different GAP concentrations.	9
Figure 8: Pictures taken after $10 \mu\text{s}$ with $4.5 \text{ J/cm}^2$ for different GAP concentrations.	9
Figure 9: Pictures taken after $10 \mu\text{s}$ with $7.4 \text{ J/cm}^2$ for 2 different GAP concentrations.	10
Figure 10: Shockwave front position versus time for different GAP concentration at $0.55 \text{ J/cm}^2$ .	11
Figure 11: Summary of the shockwave velocities measured at $1 \mu\text{s}$ .	12
Figure 12: Emission of Si nanoparticles produced by fs laser irradiation (adapted from Ref.1).	13
Figure 13: Emission spectra for GAP+C after fs laser irradiation. Spectral range (i.e. x-axis of each image) from 370 to 600 nm, while the images were recorded after 35, 135, 235, 435 and 935 ns.	14

# Ablation of viscous polymers

## *Experimental*

Four liquid solutions (including one of without GAP) plus a solid target were investigated by shadowgraphy to test whether “liquid” polymer solutions are applicable and even superior in micro laser plasma thrusters (as suggested by C.R. Phipps). Shadowgraphy was used to test whether a concentration could be identified that would behave similar to solid GAP, i.e. whether splashing - which would strongly reduce the performance of the polymer as fuel and contaminate the laser optics- can be avoided.

As solvent ethyl acetate (EA) was used, while for the absorber carbon nanoparticles (C) were applied. The following samples were prepared.

Sample	GAP content [wt%]	C content [wt%]	EA content [wt%]
Solvent	0%	1%	99%
28% GAP	28%	1%	71%
50% GAP	50%	1%	49%
70% GAP	70%	1%	29%
Solid GAP	99%	1%	0%

The liquid samples were placed on a PTFE slide and irradiated by 6 ns pulses at 1064 nm from a Nd:YAG laser (pump laser). The spot size was a circle of 300  $\mu\text{m}$  diameter. The illumination was obtained by a fluorescent dye pumped with 30 ns pulses at 308 nm from a XeCl excimer laser (probe laser). A camera with a zoom objective was used to image the process. The experimental setup is shown in Figure 1.



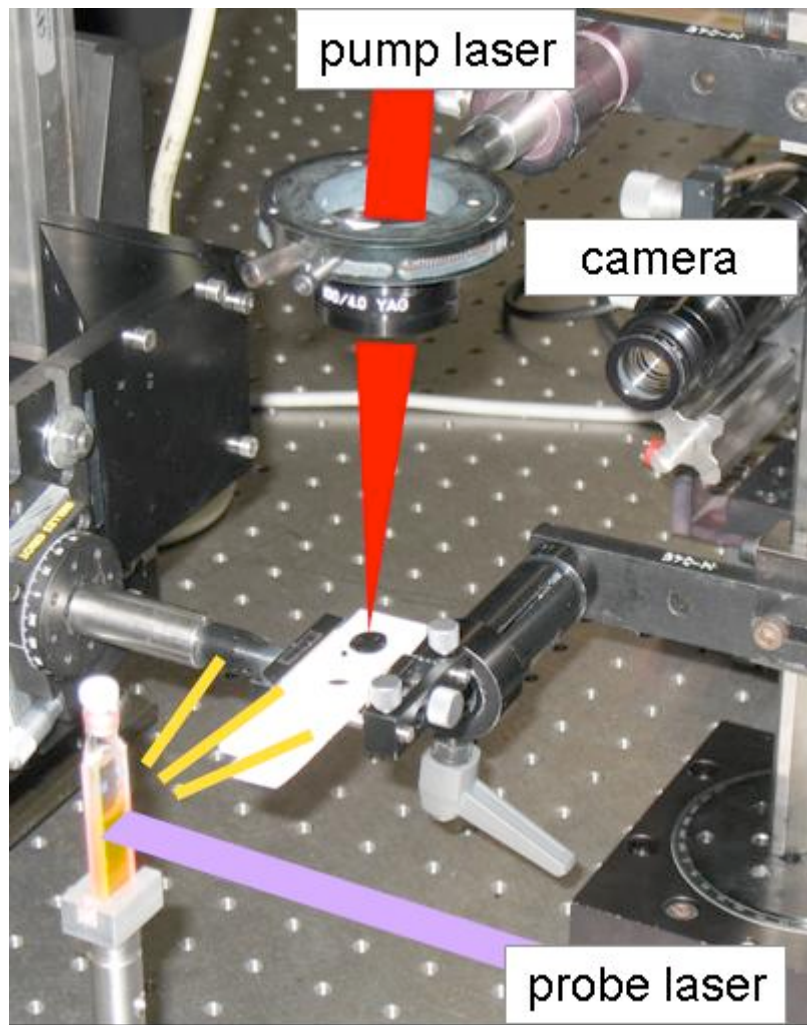


**Figure 1 : Overview of the experimental setup.**

## Shadowgraphy

Shadowgraphy was applied as experimental technique as it shows directly whether splashing is observed but also whether a solution behaves similar to solid GAP which is up to now the “best” solid fuel for laser micro plasma thruster (see previous report).

### Solid GAP

Solid Gap has been analyzed to allow a direct comparison between the viscous polymers and the solid material. The ablation of solid GAP+C targets produces a shockwave (visible at 1 and 2  $\mu\text{s}$  in Figure 2.) and the ejection of particles (at higher fluences, i.e. used for “plasma” conditions, particles cannot be observed because the plasma is too bright).

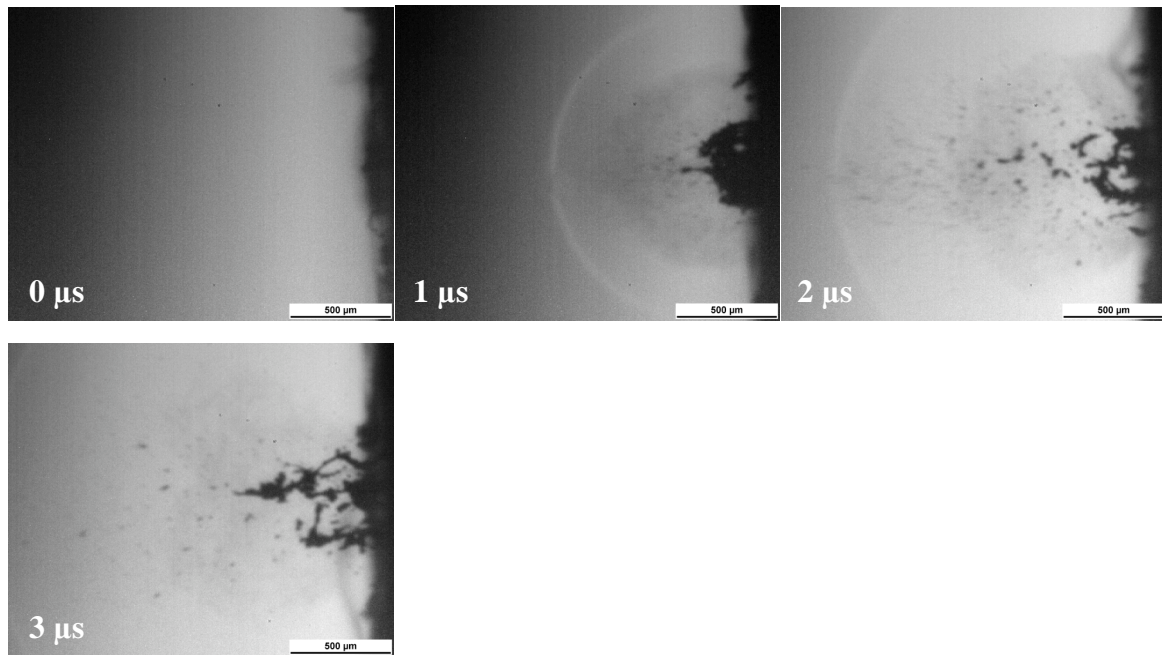


**Figure 2: Sequence of pictures taken for solid GAP with 1% C particles at 3.2 J/cm<sup>2</sup>.**

A performance similar to this behavior would be the benchmark for the “liquid” polymers.

### Ethyl acetate (solvent with carbon)

The ablation of a liquid target (pure solvent with carbon) yields a different behavior than observed for the solid GAP samples. A cloud of droplets is ejected first, but after several microseconds the liquid surface begins to collapse and jet of liquid is produced (see Figure 3). This behavior can be described as splashing. The splashing is observed for time scales longer than 200  $\mu\text{s}$ .

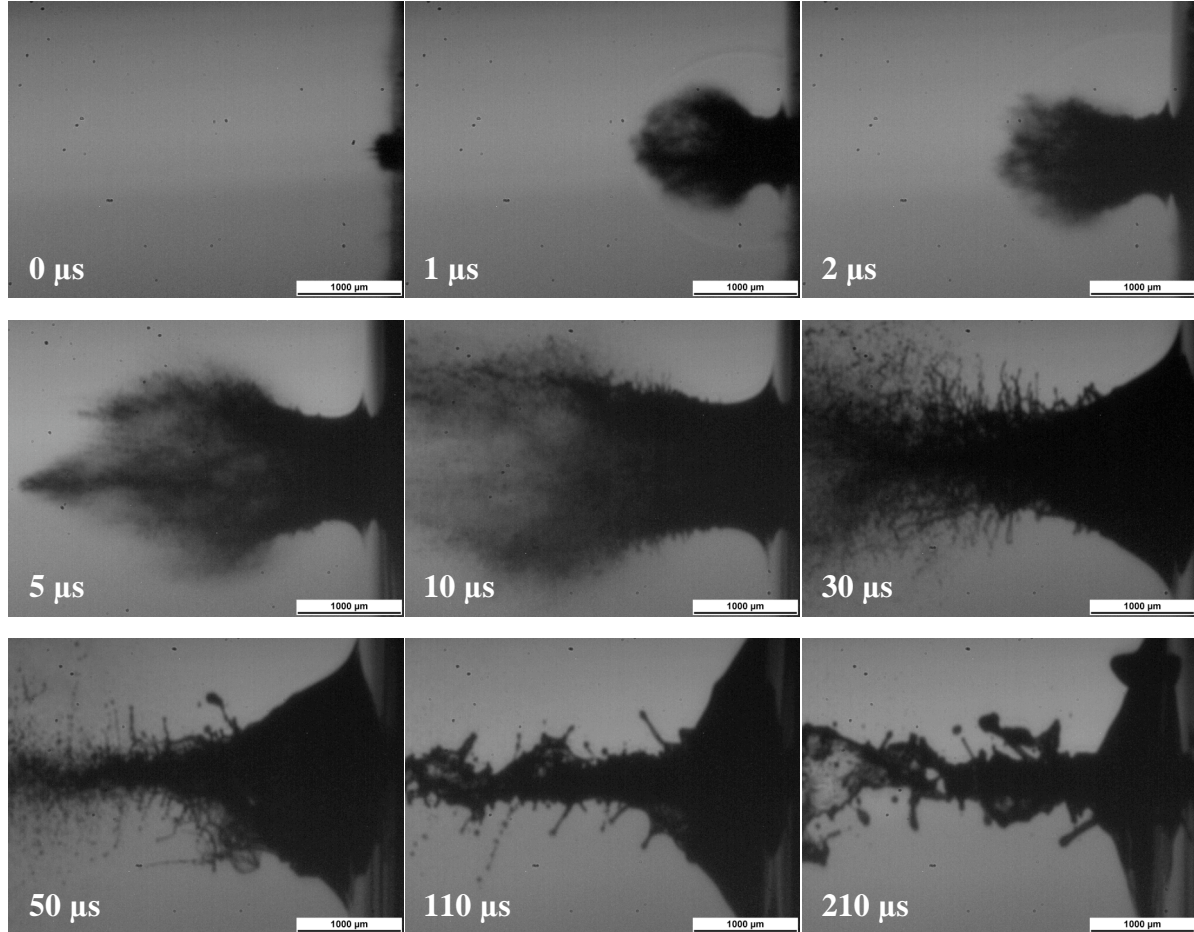


**Figure 3:** Sequence of pictures taken for ethyl acetate (solvent) with 0.7% C particles at  $2.8 \text{ J/cm}^2$ .

## Non-splashing behavior

Detailed shadowgraphy experiments reveal two possible behaviors during the ablation of liquid GAP solutions. One observed behavior is shown in the Figure 4.

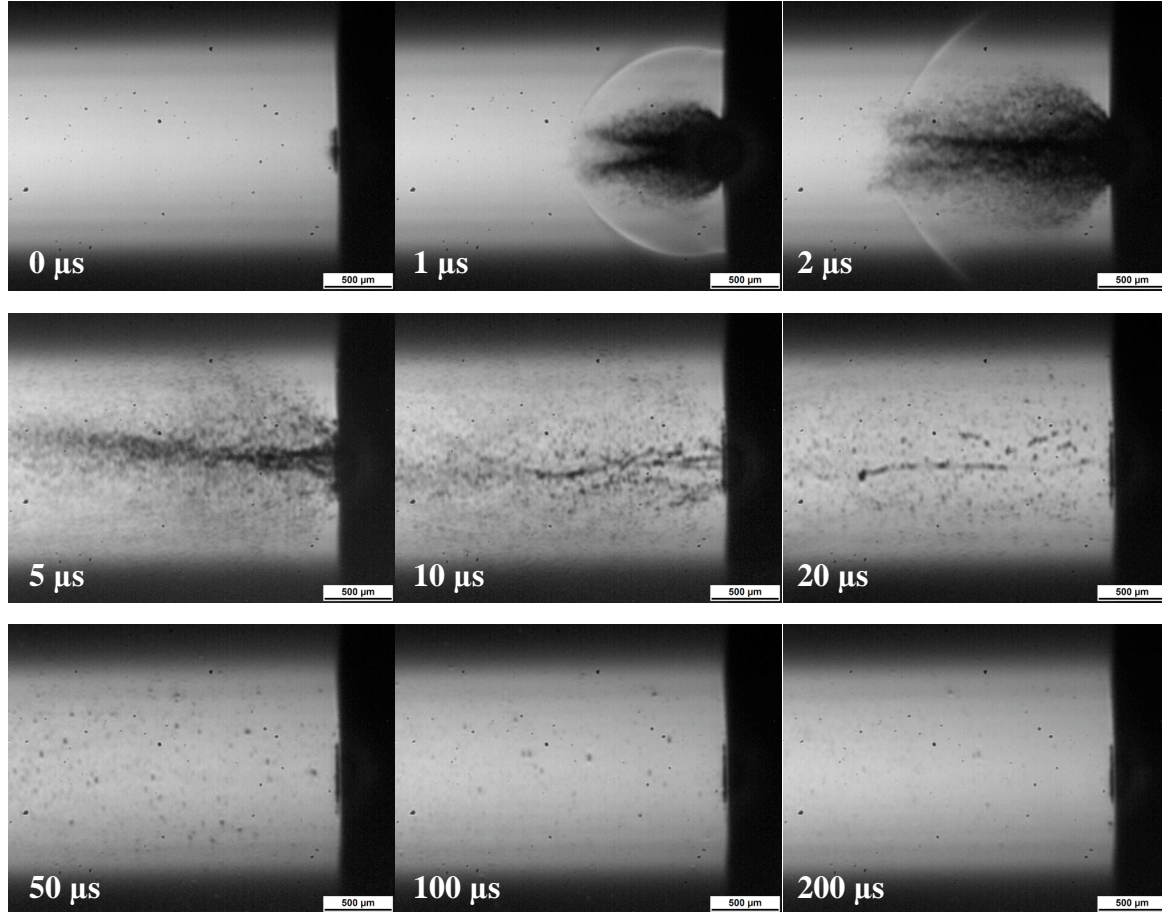


**Figure 4: Sequence of pictures taken for the 70% GAP solution at  $2.2 \text{ J/cm}^2$ .**

Within 5 μs, the material is ablated and particles are ejected. Remaining particles or droplets are still ejected until 10 to 20 μs. After this time, the ablation process is finished. This process is comparable to the ablation of solid targets, although the solid particles are faster than in the case of solid GAP, i.e. they overtake the shock wave after 1-2 μs, which is not observed for solid GAP.



## Splashing behavior

The other observed process is the removal of liquid material by splashing. Figure 5 shows the evolution of the sample and area above the sample during splashing.

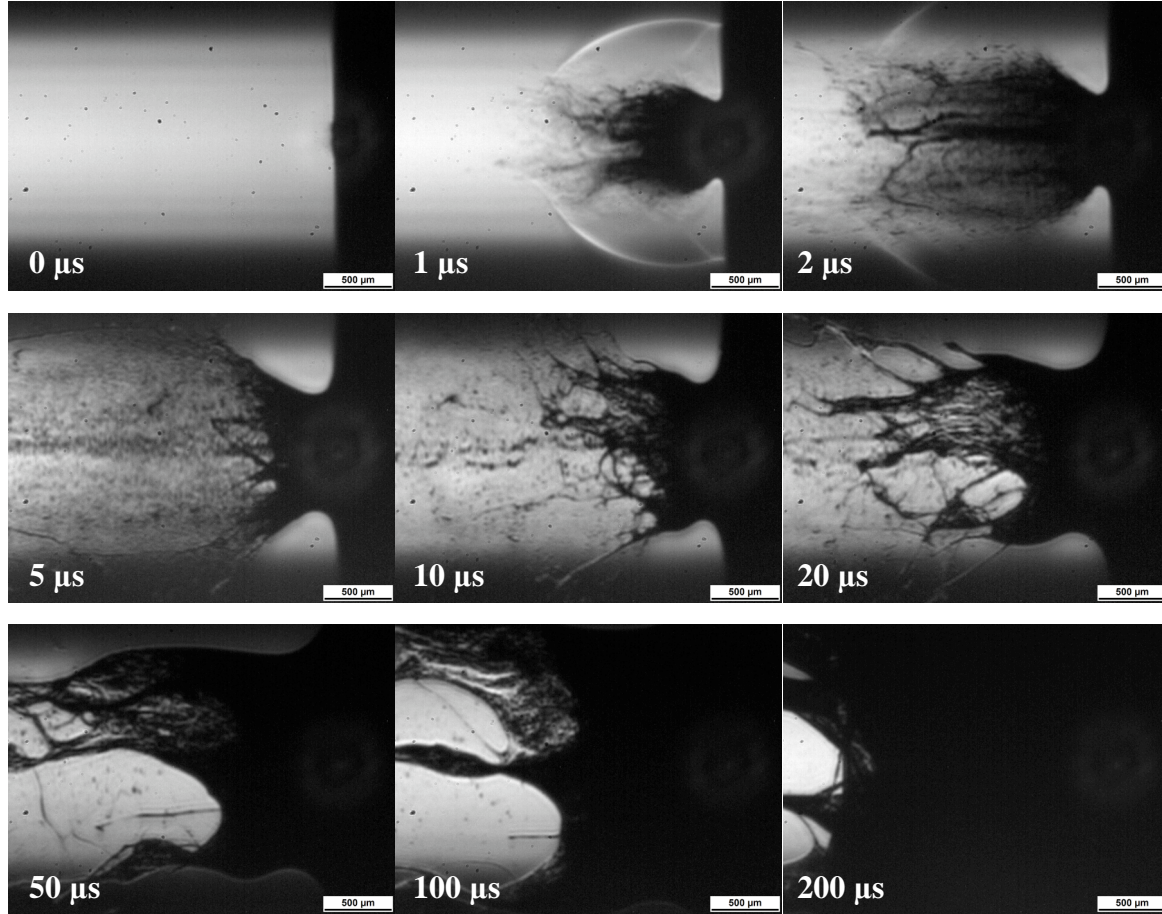
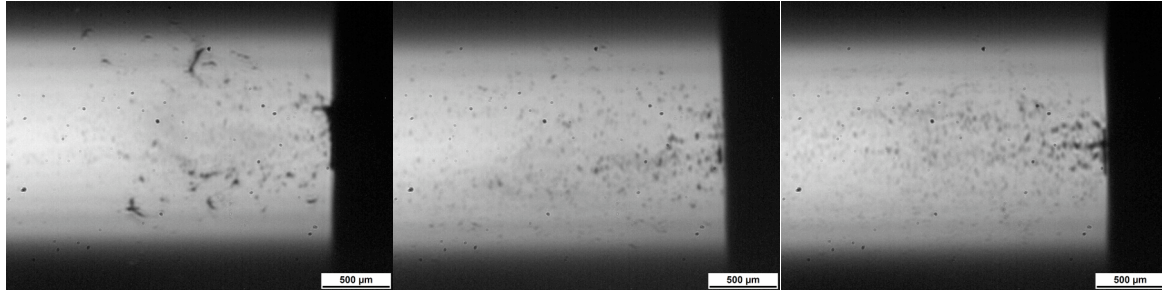


**Figure 5: Sequence of pictures taken for the 28% GAP solution at  $4.5 \text{ J/cm}^2$ .**

The very first steps are similar to the non-splashing ablation. However, two different features can be distinguished: liquid filaments are visible in the plume (which overtake the shockwave at  $2 \mu\text{s}$ ), and the base of the plume is connected to the liquid surface by a meniscus. This becomes particularly clear at  $5 \mu\text{s}$ , where the liquid surface appears similar to a liquid after impact of a solid particle. The area of the moving liquid is much larger than the original spot size of  $300 \mu\text{m}$ . After  $20 \mu\text{s}$  the surface of the liquid seems to expand to several millimeters. After  $500 \mu\text{s}$  (not shown) the liquid surface is still in an upward movement.

## Transition between the behaviors

The pictures (Figure 6) taken after 9-10  $\mu\text{s}$  were chosen to determine which of the two processes is observed.



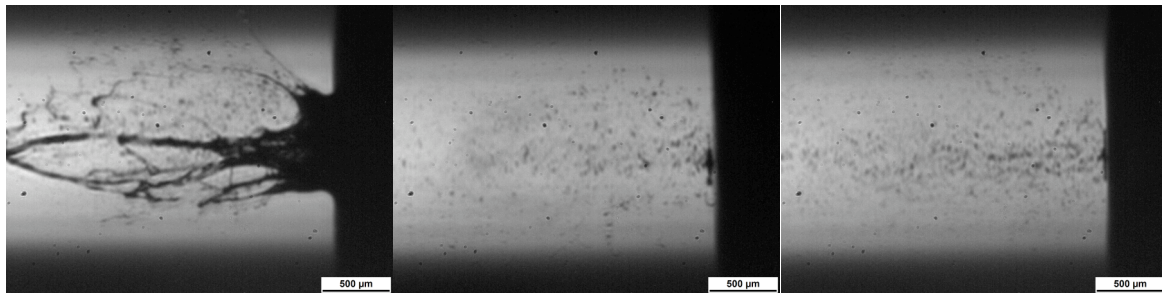
28% GAP

50% GAP

70% GAP

**Figure 6: Pictures taken after 9  $\mu\text{s}$  with  $0.55 \text{ J/cm}^2$  for different GAP concentrations.**

At low fluences, all concentrations have the same classical behavior (see Figure 7).



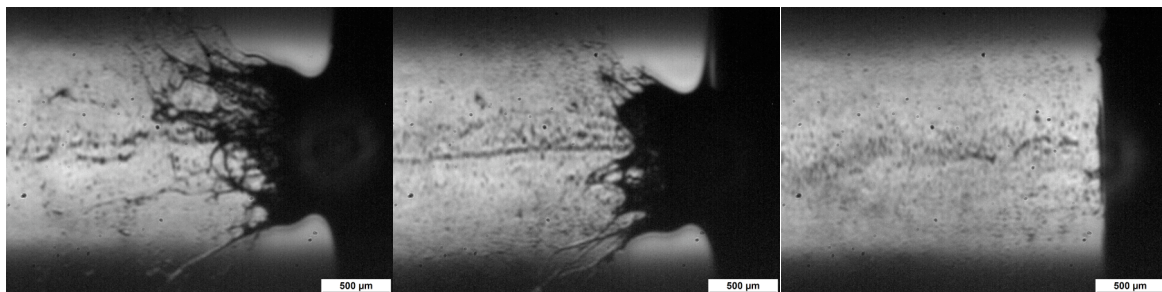
28% GAP

50% GAP

70% GAP

**Figure 7: Pictures taken after 10  $\mu\text{s}$  with  $0.8 \text{ J/cm}^2$  for different GAP concentrations.**

At higher fluences (see Figure 8), the 28% GAP, the least viscous solution, shows a splashing behavior but the two most viscous solutions do not reveal this behavior.



28% GAP

50% GAP

70% GAP

**Figure 8: Pictures taken after 10  $\mu\text{s}$  with  $4.5 \text{ J/cm}^2$  for different GAP concentrations.**

At  $4.5 \text{ J/cm}^2$ , the 50% GAP sample is splashing while the 70% GAP sample is still similar to a solid (Figure 9).

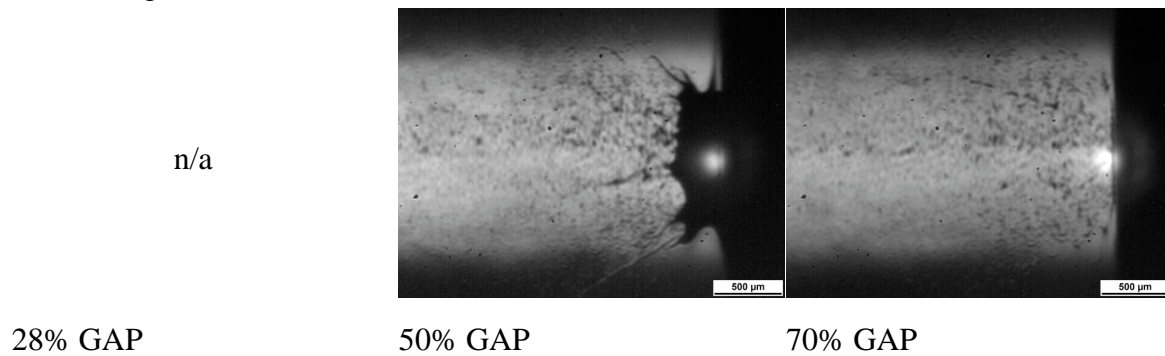


**Figure 9: Pictures taken after  $10 \mu\text{s}$  with  $7.4 \text{ J/cm}^2$  for 2 different GAP concentrations.**

The 70% GAP sample still reveals the non-splashing behavior at the highest applied fluence, where the plasma onset is already observed (bright spot in the pictures) close to the laser-liquid interaction zone.

For a given concentration of GAP, there is a transition between the solid-like mode and the splashing mode when the fluences are increased. There is also a clear relation between the concentration of the solution and the fluence at which this transition occurs. For solutions with a lower concentration, a lower transition fluence is observed. For the 70% concentration, this transition is not observed in the investigated fluence range, showing that this concentration behaves similar to solid GAP.

## Shockwave velocities

The shockwaves produced by the ablation can also yield information on the released energy during the process. Shockwave evolution versus time was measured for the three GAP solutions. From these data, the velocity at 1  $\mu\text{s}$  was calculated and compared to the velocities of the solid GAP and pure solvent. An example of the evolution of the shockwave front is given in Figure 10.

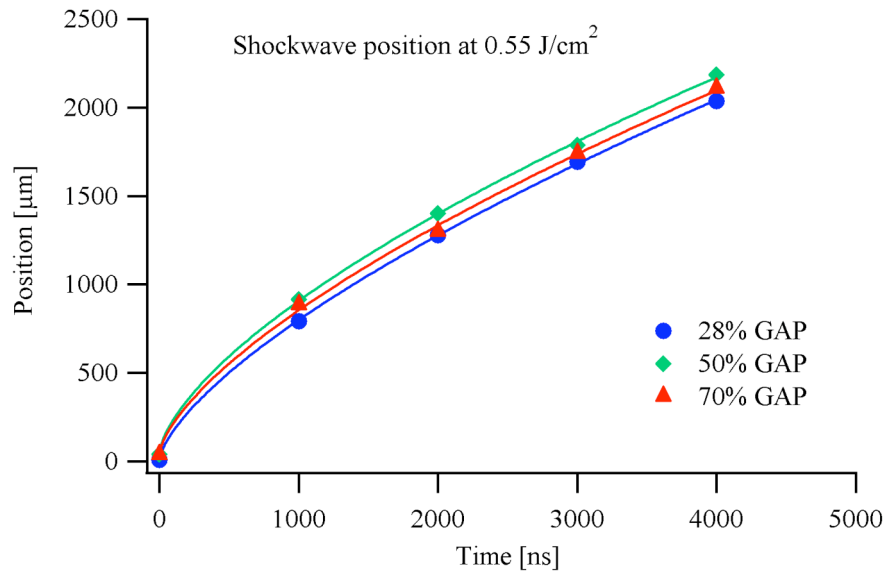


**Figure 10: Shockwave front position versus time for different GAP concentration at 0.55 J/cm<sup>2</sup>.**

The position evolution is fitted by a power law,

$$x(t) = a + b \cdot t^c$$

x	position
t	time
a, b, c	fit parameters

The velocity at 1  $\mu\text{s}$  is obtained by the value of the fit derivative at this time. A summary of all velocities is given below in Figure 11.



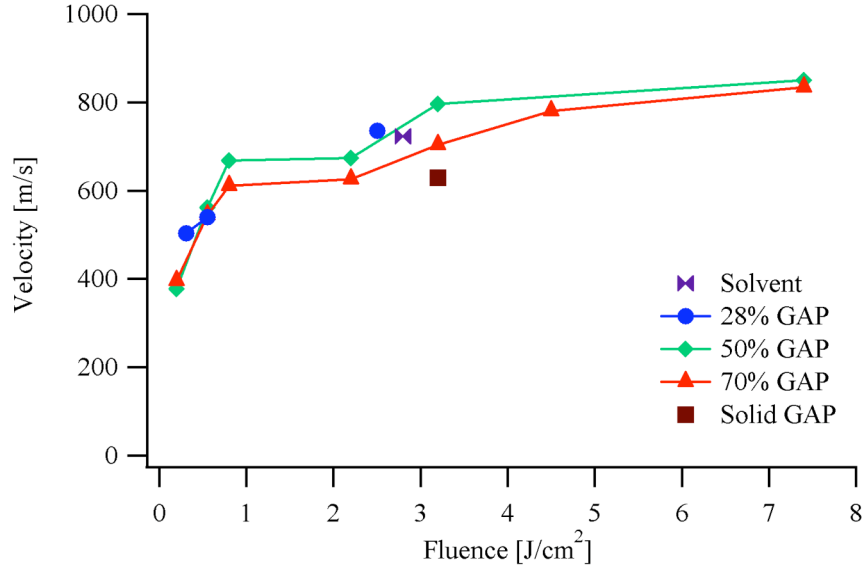


**Figure 11: Summary of the shockwave velocities measured at 1  $\mu$ s.**

The shockwave velocity increases with increasing fluence, which is an expected result. This increase is steeper close to the threshold fluence (low fluence range) than for the rest of the investigated domain.

The influence of the GAP concentration is less clear. For a given fluence, all samples have comparable shockwave velocities. However, a slight trend arises from the plot: the higher the GAP content in the target, the slower the shockwave. This result is not really expected, and a possible correlation of the splashing transition with the velocities is not possible.

One possible explanation for this effect may be related to the boiling points. The solvent is readily vaporized and therefore more energy can be released by the shock wave, yielding faster shock waves for samples with higher solvent content.

These data suggests also clearly that GAP solution with a concentration of  $\geq 70\%$  of GAP can be applied as fuel in micro laser plasma thrusters.

To quantify these results in more details the viscosity of the solutions has been measured, showing the pronounced differences are observed.

Solution	Dynamic viscosity [Pa s]
28% GAP	0.012
50% GAP	0.46
70% GAP	14

The three solutions have very different rheological properties, as the dynamic viscosity increases very fast for GAP concentrations  $> 50\%$ . It appears that the required viscosity to apply liquid GAP solution as fuel for micro laser plasma thruster is above 10-15 Pa s approximately.

## Carbon nanoparticle during/after plasma formation with fs laser irradiation

We have reported in the final report of our previous project *Polymers used as Fuel for Laser Plasma Thrusters in Small Satellites* (contract FA8655-03-1-3058) about the plasma formation in energetic polymers such as GAP after irradiation with fs laser pulses at a wavelength of 800 nm. One of the remain question in this study was related to the existence of 3 different components in the data from plasma plume imaging. The first two components could be clearly assigned by plasma spectroscopy to atomic ions and neutral and diatomic species, while the spectroscopy data for the longer time scales (i.e. the 3<sup>rd</sup> component were missing). We speculated that this third component may be due to nanoparticle emission which has been reported previously<sup>1</sup> for fs laser irradiation of silicon (see Figure 12).

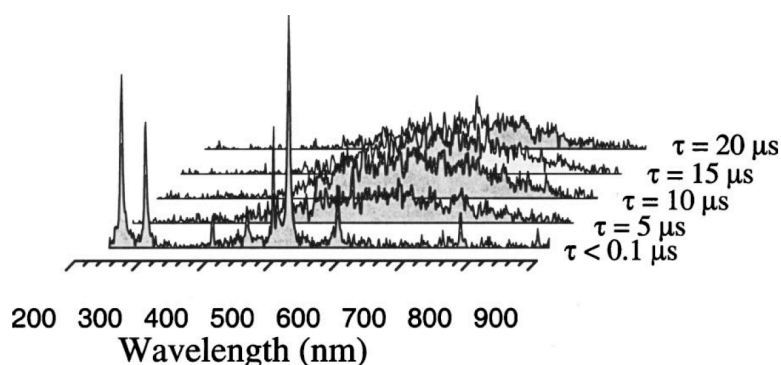


**Figure 12: Emission of Si nanoparticles produced by fs laser irradiation (adapted from Ref.1).**

The most important feature of nanoparticle emission is the broad band emission of the nanoparticles for longer time scales. We have performed the missing experiments (experimental setup has been described in detail in the previous report) to prove nanoparticle emission in the case of fs irradiation of GAP doped with carbon. A laser energy of 300  $\mu\text{J}$  was used with 10 pulses per position in the time scale where plasma imaging has revealed the third component. The time resolved spectra in Figure 13 show clearly that this component which becomes clearly visible after 235 ns have the typical broad band emission features of nanoparticles. As these features are only observed in the case of carbon doping (and not for an IR dye) we can conclude the particles are consist most probably of carbon originating form the carbon dopant. The earlier observation time for the nanoparticles from GAP+C compared to the Si nanoparticles in Si are most probably due to the different material properties and laser fluence.

---

<sup>1</sup> S. Amoruso, R. Bruzzese, N. Spinelli, R. Velotta, M. Vitiello, X. Wang, G. Ausanio, V. Iannotti, and L. Lanotte, *Generation of silicon nanoparticles via femtosecond laser ablation in vacuum*, Appl. Phys. Lett., 84 (2004) 4502-4504.

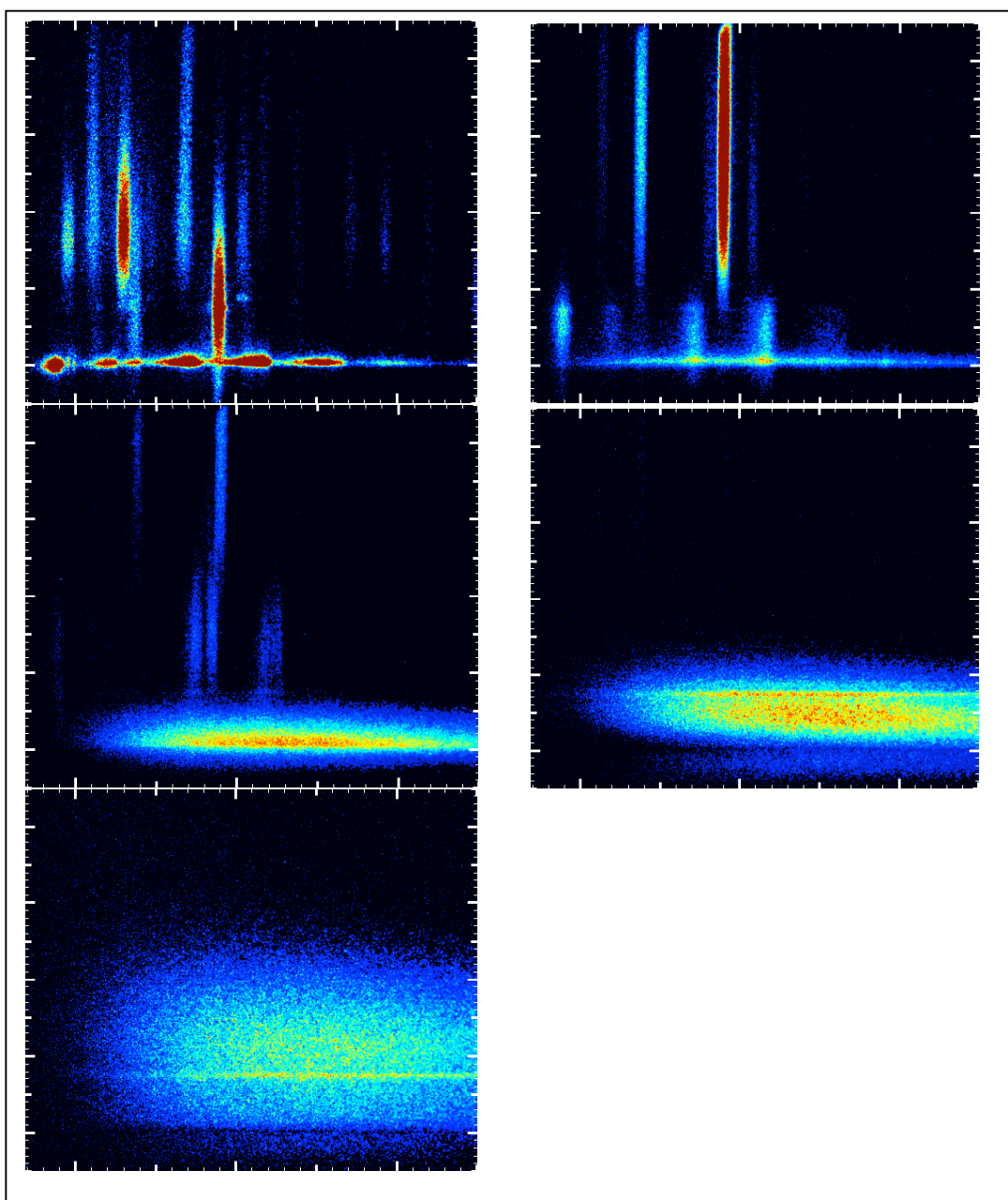


**Figure 13: Emission spectra for GAP+C after fs laser irradiation. Spectral range (i.e. x-axis of each image) from 370 to 600 nm, while the images were recorded after 35, 135, 235, 435 and 935 ns.**

## **Preparation of publication from previous project**

The publication on the fs laser interaction and plasma formation on the various tested polymers has been prepared and is at the moment with our co-authors for final comments. The paper will be submitted in January to *Plasma Processes and Polymers*.